BOREAL ENVIRONMENT RESEARCH 27: 131–144
ISSN 1797-2469 (online)

Helsinki 15 September 2022

Two-decade variability of climatic factors and its effect on the link between photosynthesis and meteorological parameters: example of Finland's boreal forest

Larysa Pysarenko[1)]*, Svitlana Krakovska[1)], Mykhailo Savenets[1)], Ekaterina Ezhova[2)], Anna Lintunen[2)3)], Tuukka Petäjä[2)], Jaana Bäck[3)] and Markku Kulmala[2)]

[1)] *Ukrainian Hydrometeorological Institute (UHMI), Kyiv, Ukraine, (*corresponding author's e-mail: larpys@uhmi.org.ua)*
[2)] *Institute of Atmospheric and Earth System Research (INAR/Physics), University of Helsinki, Helsinki, Finland*
[2)] *Institute of Atmospheric and Earth System Research (INAR/Forest sciences), University of Helsinki, Helsinki, Finland*

Received 25 Jan. 2022, final version received 24 Aug. 2022, accepted 22 Aug. 2022

Pysarenko L., Krakovska S., Savenets M., Ezhova E., Lintunen A., Petäjä T., Bäck J. & Kulmala M. 2022: Two-decade variability of climatic factors and its effect on the link between photosynthesis and meteorological parameters: example of Finland's boreal forest. *Boreal Env. Res.* 27: 131–144.

Climate and forests are linked to each other via sophisticated feedback mechanisms. Recognizing the complexity of atmosphere-biosphere interactions, here we use a simplified approach aiming to establish connections between the parameters characterizing the boreal forest as a carbon sink and meteorological parameters using a two-decade data set (1996–2017) from the Station for Measuring Ecosystem — Atmosphere Relations (SMEAR II), Finland. First, we quantify climate changes in Finland using growing season length and climatic indices. Then we apply the indices to determine unusually cold, warm, wet, or dry years as compared with the typical conditions at SMEAR II. Further, we analyze the relationships between air temperature, precipitation, absorbed photosynthetically active radiation (PAR) and atmospheric CO_2 concentration. Our results suggest increased photosynthesis in the Finnish boreal forest with warming and emphasize the importance of long-term measurements for integrated atmosphere-biosphere studies.

Introduction

Forests cover 30% of total land area and play an important role in global climate: they affect regional climate via surface roughness, albedo, and atmospheric concentration of greenhouse gases, most importantly carbon dioxide (CO_2) (Bonan 2008, Findell *et al.* 2009, Sanderson *et al*. 2012, Arneth *et al.* 2016). At the same time, forests are vulnerable to climate change, which causes timberline shifts, invasion of pests etc. (Menzel *et al.* 2006, IPCC 2007, IPCC 2013, Matías and Jump 2014, Thom *et al.* 2017, IPCC 2018, IPCC 2019a). All these processes contribute to complex atmosphere–biosphere interactions and feedbacks, which vary under climate change.

Editor in charge of this article: Veli-Matti Kerminen

The boreal forest belt covers an area between 50°N to 70°N, constituting 33% of the whole area occupied by forests on the planet (Gauthier *et al.* 2015; Global forest atlas). The northern regions are warming twice as fast as the global average (IPCC 2019b). It is expected that the average air temperature will increase up to 2°C by the end of the 21st century and will cause a positive effect on vegetation, enhancing forest productivity in the northern temperate and boreal vegetation zones, but further warming to 3–4°C can have a negative effect due to e.g., increasing water deficit (D'Orangeville *et al.* 2018). Accordingly, many models have shown a negative correlation between air temperature increase and forest development in some regions, indicating difficulties in ecosystems' adaptation (Bonan and Sirois 1992, Ruosteenoja *et al.* 2016, Babst *et al*. 2019, Larjavaara *et al*. 2021).

Forests and climate conditions interact via direct and indirect complex connections. Air temperature (T) is a limiting factor for forest ecosystem productivity in high latitudes influencing e.g., timing of different phenological stages. In addition, saturation vapor pressure exponentially depends on temperature, thus increasing T at a constant water vapor concentration in the air leads to an increase of vapor pressure deficit. Too high water vapor pressure deficit dampens evapotranspiration and photosynthesis rate (Rawson *et al.* 1977, Massmann *et al.* 2019). According to Bonan (2008), boreal evergreen forests have low albedo and their effect on the local temperature in this respect is rather warming. However, there are competing processes that can counteract the albedo effect (Kulmala *et al.* 2020). The forests have the ability to cool the climate. First, they take up CO_2 during photosynthesis and store it in plant biomass and soil. Second, emissions of volatile organic compounds from forests lead to formation and growth of secondary atmospheric aerosol particles, which redistribute solar radiation and influence cloud formation and carbon sink (Arneth *et al.* 2016, Kulmala *et al.* 2020). Third, released water vapor due to transpiration from plants can condense and induce cloud formation and rain (Teuling *et al.* 2017, Pauli *et al.* 2022, Petäjä *et al.* 2022, Räty *et al.* 2022). Clouds effectively reflect and scatter incoming solar radiation due to high albedo. Via their effects on surface roughness, forests induce aerodynamic effects: trees slow down the wind speed within the canopy but strengthen turbulence above them (Sanderson *et al.* 2012). Kulmala *et al.* (2020) estimated recently that in Northern Europe, cooling aerosol-induced effects of the boreal forest on clouds and carbon sink could compensate for the warming effect due to albedo. More research is needed to resolve the net effect of boreal forests on the climate.

Boreal forests play an important role in the carbon cycle acting as carbon storage and sink. In general, boreal ecosystems contain approximately 27% of all carbon stored in the world's vegetation (biomass) and 50% of carbon stored in soils (Alonzo *et al.* 2018). CO_2 fluxes from soils, which strongly depend on soil temperature, can also be affected by the amount of precipitation. Makhnykina *et al.* (2018) found that CO_2 fluxes exhibit a significant exponential dependence on soil temperature during growing seasons. Increase in precipitation may inhibit and intensify the rate of CO_2 fluxes from the soil during the active growing season when air temperature was above 10°C (Makhnykina *et al.* 2018). Related to fixation of CO_2 into tree biomass, the rise of air and surface temperatures in combination with the increase of atmospheric CO_2 concentrations influence the photosynthetic activity (Fernández-Martínez *et al.* 2017). In addition, there is an effect of CO_2 fertilization, which is related to the increase in plant biomass or leaf area index (LAI). Bigger leaf mass can also decrease albedo (Palmroth 2009).

In Finland, forests cover about 75% of its land area with prevailing species of Scots pine, Norway spruce and two birch species (Majasalmi 2015). In some recent years, they have absorbed even more CO_2 than emitted by the country thus compensating total CO_2 emissions (OSF 2017, Björheden 2021). Vegetation (growing) season usually begins when daily mean temperature exceeds +5°C and varies from 180 days in the south-west of Finland to 100–140 days in Lapland (Rousi and Heinonen 2007; FMI). According to climate projections, the rise of air temperature and precipitation is expected especially in boreal Finland in winter (Kinnunen *et al.* 2013, Ruosteenoja *et al.* 2016). As a result, the growing season will extend by up to 40–50 days by 2100 (Ruosteenoja *et al.* 2011). The increase in integral parameters representing accumulation of heat, such as sums of air tem-

perature (growing degree-days, depending both on mean temperature and length of the growing season) will stimulate more intensive growth and particularly, vegetation shift to development of deciduous forest (Kinnunen *et al.* 2013).

Despite substantial progress in understanding the forest-atmosphere interactions, there are many gaps that need to be addressed. In this study, we aim to investigate interactions between parameters characterizing boreal forest as a carbon sink and meteorological parameters using data sets from a well-equipped forestry field station, SMEAR II (Station for Measuring Ecosystem-Atmosphere Relations, Hyytiälä), in southern Finland. We use climatic indices to study the effect of climate change on boreal forests. These indices allow distinguishing between cold/warm and humid/dry years, thus providing relevant information for analysis of the interaction between atmosphere and absorbed photosynthetically active radiation (PAR). Absorbed PAR is used as a proxy for photosynthesis and we study its relation with air temperature and CO_2 concentrations. In other words, we utilize a simplified approach to study the effect of climate change on photosynthesis using parameters that are measured in many sites or can be calculated based on these parameters. The aims of the present study are as follows: 1) quantify the climate change effects at SMEAR II using climatic indices and explore their ability to reflect air temperature and precipitation variability; 2) study the connections between PAR and air temperature; 3) explore relation between PAR absorbed by the forest canopy and atmospheric CO_2 concentration; and 4) analyze the influence of air temperature on PAR absorption and atmospheric CO_2 concentration.

Material and methods

Studied area and initial meteorological data

The SMEAR II forestry field station at Hyytiälä (61°51′N, 24°17′E, 180 m above sea level) has been operating since 1995 (Hari and Kulmala 2005). It is situated in southern Finland in the boreal zone. The typical climatic conditions for this station are as follows (Kolari *et al.* 2007): the mean annual temperature is +3.3°C; mean annual precipitation is 713 mm; date of snowmelt is the 30th of April; the mean length of growing season is 162 days. The average density of the forest is ca. 1170 trees ha^{-1} and basal area (in 2006) 24.3 m^2 ha^{-1}. The canopy is mainly formed by *Pinus sylvestris* (75%), with some subordinate *Picea abies* (15%) and broadleaf trees (10%) such as *Betula pendula* and *Sorbus aucuparia*. Understory vegetation consists of e.g., ericoid shrubs such as lingonberry (*Vaccinium vitis-idaea* L.) and bilberry (*Vaccinium myrtillus* L.), mosses such as *Dicranum* sp, and grasses such as *Deschampsia flexuosa* (Ilvesniemi *et al*. 2009, Mäki *et al*. 2019a, Mäki *et al*. 2019b). A mild forest thinning was done at the area of interest in 2002 (Vesala *et al.* 2005). The pine foliage is located in the upper third of the canopy height. The measurements at SMEAR II include observations of different parameters in soil, water, vegetation, and atmosphere to study atmosphere-biosphere interactions (Hari *et al.* 2005; SMEAR concept).

We used hourly data from an open research data portal SmartSMEAR (https://smear.avaa.csc.fi/) for all available periods of measurements: air temperature at the height of 4.2 m from 1996–2017, photosynthetic active radiation (PAR) at 0.6 m (below the canopy), 18 m (at the top of the canopy), reflected PAR (67 m) from 2004–2017, precipitation from 2005–2017 and CO_2 concentration at 4.2 m from 1996–2017. For 1996–2004, the data was taken from Finnish Meteorological Institute weather station next to the SMEAR II. We averaged air temperature and PAR to get their daily values and summed up precipitation.

There were gaps in the air temperature data set (see Supplementary Information Table S1). Depending on the length of missing data at the height of 4.2 m, three methods were used for gap filling. The first approach applied to cases where missing data periods were short, from one to three days. We averaged the neighboring data:

$$T = \frac{\sum_{i=1}^{n/2} (T_{db} - i^{+T} de + i)}{n}, \quad (1)$$

where n is the number of days with missing data ($n = n + 1$ if n is odd); T_{db} and T_{de} are daily air

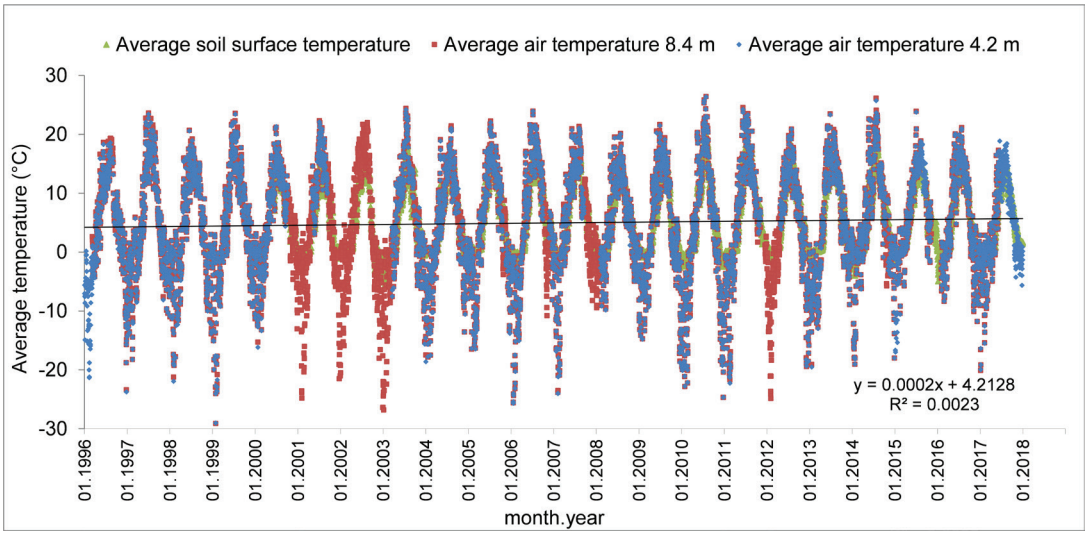

Fig. 1. Time series of the daily mean air temperature for 4.2 m (blue), partially recovered from the data at 8.4 m (red) and surface (green).

temperatures before the first (begin) and after the last (end) days of a gap, respectively.

In the second case, when gaps in time series at height of 4.2 m covered more than three days, we used data from another sensor from the height of 8.4 m. Before filling in the missing data, we checked their coherence by comparing available air temperature at both heights. We confirmed the consistency of the air temperature time series at heights of 4.2 m and 8.4 m as the average difference between them was only 0.3°C and the Pearson correlation coefficient was 0.99. In the third case, when there was a significant data gap at 4.2 m (Table 1) and 8.4 m, it was replaced with surface air temperature (Fig. 1).

Indices and comprehensive indicators

There are plenty of indices that are used for estimates of climate-forest interactions: stable air temperature transitions through 0, 5, 10, 15°C and duration of these seasons; sum of temperatures over 0, 5, 10, 15°C; sum of effective temperatures (0, 5, 10, 15°C); biotemperature (which is calculated using annual sum of positive mean temperatures divided into 365 days); the sum of negative air temperatures; soil frost depth; sums of precipitation; hydrothermal coefficients etc. (Shvidenko *et al.* 2017; Shvidenko *et al.* 2018). Fraction of Absorbed Photosynthetically Active Radiation (FAPAR) is included to the list of Essential Climate Variables for biosphere by WMO as it is a main driver of photosynthesis (see details at).

In the present study, we use climatic indices related mainly to the warm season ($T > 0$°C). They are defined in Table 1. To study biosphere-atmosphere interactions, we chose the annual cycle of absorbed PAR because it is connected to carbon uptake, characterized by gross primary production (GPP). To calculate PAR absorbed by the forest canopy, we used the following equation:

$$PAR_{absorbed} = PAR_{18m} - PAR_{0.6m} - PAR_{reflected}, \quad (2)$$

where PAR_{18m} is measured at the top of the canopy (18 m), $PAR_{0.6m}$ below the canopy (0.6 m) and $PAR_{reflected}$ is the reflected radiation at 67 m (this parameter has gaps in observations from 29.08.2011 to 4.10.2017). Absorbed PAR is presented using both absolute values (μmol m^{-2} s^{-1}) and as percentage of incoming PAR at the upper height (%). Pearson correlation coefficient was used to analyze the dependence between air temperature, atmospheric CO_2 concentrations and absorbed PAR.

Table 1. Climate indices used in the study period from 1996–2017

Index	Interpretation	Description/Formula
1. Dates of steady air temperature transitions through 0°C, 5°C and 10°C in spring and autumn	Detection of warm season (above 0°C), growing season (above 5°C), and season of active vegetation (above 10°C) for further estimates of temperature accumulation	According to Fedorov's method (Skrynyk and Snizhko 2008), the date of steady air temperature transition through the defined temperature threshold is the day when the sums of positive deviations start to exceed the sum of negative ones as temperature rises (and vice versa as it decreases).
2. Duration of seasons (D_s)	Length of the warm, growing and active vegetation seasons	D_s is the number of days between autumn and spring days of relevant temperature transition below/above the temperature thresholds
3. Sums of growing degree-days (GDD) for the above-mentioned seasons ($T_{av(>0,\ 5,\ 10°C)}$), also known as degree-days for the above-mentioned seasons	Integrative index for determination of heat accumulation	$$\sum T_{av(>0,5,10°C)} = \sum_{i=1}^{n} T_{av} > T_{\text{threshold}},$$ where T_{av} – average daily air temperature; n – a number of days between defined thresholds (0°C, 5°C, 10°C) when T_{av} exceeded temperature of threshold ($T_{threshold}$)
4. Sum of precipitation for warm season (0°C), growing season (5°C), season of active vegetation (10°C) (R_T)	Indication of dry and wet years, for further calculation of specified indices	$\Sigma P_{Tav\ (0,5,>\ 10°C)}$, where P is daily precipitation
5. Vorobyev's hydrothermal coefficient (T, W)	Heat (T) and moisture (W) resources for tree growth T has 7 gradations (λ, a–f): from extremely cold (λ) to warm climate (f). W has 6 intervals (0–5): from extremely dry conditions W = < –0.8 (marked 0) to wet climate W > 4.8 (5)	$$T = \frac{\sum T_{av>0}}{30}$$ $\Sigma T_{av\ >\ 0}$ – sum of GDD; 30 – number of days in month $$W = \frac{\sum P_{T>0}}{\sum T_{av>0}} - 0.0286 \sum T_{av>0},$$ where $\Sigma P_{T>0}$ – sum of precipitation taken for warm season; T – sum of monthly temperatures above 0°C.
6. Selyaninov's hydrothermal coefficient (HTC)	Moisture resources for plants during active vegetation season The gradation of HTC is as follows (Čirkovs 1978): - HTC > 2.0 – very humid; - HTC from 1.0 to 2.0 — sufficiently humid; - HTC < 1.0 — insufficient humidity; - HTC from 1.0 till 0.7 — dry; - HTC from 0.7 till 0.4 — very dry	$$\text{HTC} = \frac{10 \times \sum P_{T>10}}{\sum T_{T_{av}>10}},$$ where $\Sigma P_{T>10}$ – sum (in mm) of daily precipitation for period with $T_{av} > 10°C$ (season of active vegetation); $\Sigma T_{Tav\ >\ 10°C}$ – the sum of GDD in °C.

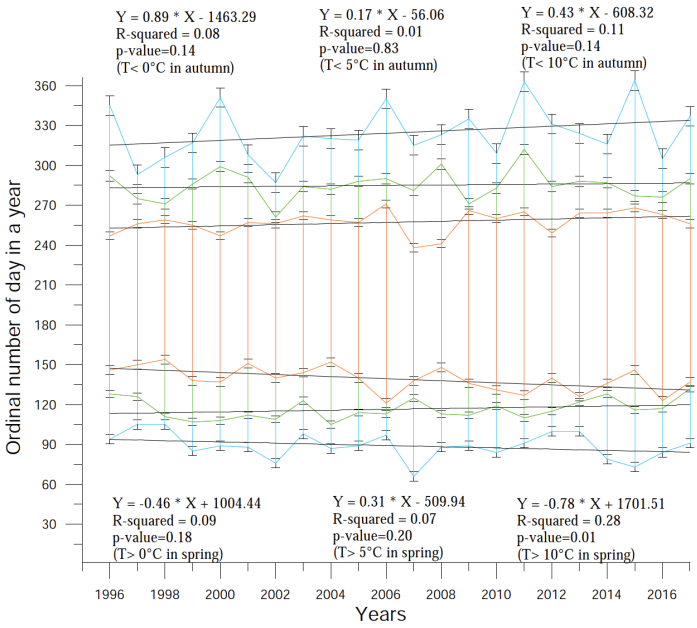

Fig. 2. Start/end dates and length of the warm season (blue), vegetative season (green) and season of active vegetation (red) with regression equations for every set of transition dates over 0°C, 5°C and 10°C with respective CI 90%.

Results and discussion

Air temperature, precipitation, and climatic indices

The calculated 22-year-long trends in the start dates, end dates and lengths of warm season, growing season and season of active vegetation are presented in Fig. 2. Variability in all indices was high, and most of the trends for the start/end date of the seasons were not statistically significant ($p > 0.05$). Slight changes were observed for the warm season with an advanced start date in spring and a delayed end date in autumn, leading to lengthening of the warm season ($T > 0$°C) at a rate of 13 days/decade. This is approximately twice the rate estimated by Ruosteenoja *et al.* (2011), reporting the season extension up to 40–50 days by 2100.

The only significant correlation was found for the earlier start of the active vegetation season ($T > 10$°C) with the trend of 7–8 days per decade. In comparison, Pulliainen *et al.* (2017) found that spring recovery of carbon uptake was advanced in 1979–2014 in a boreal region by 2.3 days per decade. However, we found that the start of the vegetation season ($T > 5$°C) was shifted to later dates with a trend of about 3 days per decade. As a result, the period with air temperature between 5°C and 10°C shrank notably, indicating that the most active growing season started earlier but the transition from the vegetation season to the most active growing season was faster. Note that the start of winter season ($T < 0$°C) had the highest variability with a confidence interval CI = 7.3 days (Fig. 2, Table 2).

All mentioned shifts for different seasons increased available heat resources and affected the rate of heat accumulation, which might influence plants' adaptation due to changes of CO_2 absorption and photosynthesis rate.

Vertical color lines in Fig. 2 correspond to the lengths of periods when daily air temperature is higher than the defined thresholds of 0°C, 5°C and 10°C, giving a possibility to compare the season lengths. The variance of season lengths was rather high and sometimes led to unfavorable conditions for plant growth with both extremely low and extremely high heat accumulation. The longest warm season of 291 days with an average daily air temperature (T_{av}) > 0°C occurred in 2015, $T_{av} > 5$°C with 202 days in 2011, and $T_{av} > 10$°C with 150 days in 2006. The shortest seasons with $T_{av} > 0$°C and $T_{av} > 5$°C were in 1997 with 188 and 149 days respectively and $T_{av} > 10$°C with 93 days in 2008 (see Supple-

mentary Information Table S2). 90% confidence intervals (CI) for air temperature transition dates as well as seasons' lengths are reported in Supplementary Information Table S2.

Sums of daily temperatures and precipitation for the studied seasons with defined temperature thresholds of 0°C, 5°C and 10°C are presented in Supplementary Information Table S2. The annual sums of daily temperatures for different seasons presented since 1996 had a strong variability with CI of 60°C (T > 0°C), 56°C (T > 5°C), and 82°C (T > 10°C) and the annual sums of precipitation had CI of 36.1 mm, 33.2 mm, 27.2 mm. The hydrothermal Vorobyev and Selyaninov indices (see Table 1 for the definitions and Table 2 for results) showed that year 2006 was extremely dry and warm (W = 2.6 and HTC = 1.0), whereas year 2008 was relatively cold and wet (W = 8.1 and HTC = 3.4). The highest W = 8.3 was in 2017 due to the wet and coldest warm season since 1996, notwithstanding that the length of all seasons exceeded their mean values. Note, that year 2011 represented rather typical meteorological conditions for humidity in the region with W = 5.0 and HTC = 2.5, but with warm conditions during the season with T_{av} > 0°C (see Supplementary Information Table S2).

Some regularities in accumulated temperature and precipitation can be observed in Fig. 3. The increase and decrease of temperature varied from year to year at the beginning of the research

Table 2. Vorobyev and Selyaninov hydrothermal coefficients from 1996–2017

Year	Vorobyev HC		Selyaninov HTC
	Sum of GDD (T_{av} > 0°C)	Index of climate humidity, W (T_{av} > 0°C)	(T_{av} > 10°C)
1996	70^{cold}	4.8	1.9
1997	70^{cold}	4.2	1.8
1998	67^{cold}	7.0^{wet}	2.8^{wet}
1999	77	3.3^{dry}	1.2^{dry}
2000	78	5.1	1.9
2001	76	5.7	2.4
2002	79	1.5^{dry}	1.2^{dry}
2003	74	4.2	1.5
2004	72	5.4	2.6
2005	78	4.2	2.3
2006	84^{warm}	2.6^{dry}	1.0^{dry}
2007	76	3.2^{dry}	1.6^{dry}
2008	70^{cold}	8.1^{wet}	3.4^{wet}
2009	72	4.2	1.6
2010	79	4.5	2.0
2011	87^{warm}	5.0	2.5
2012	71	7.6^{wet}	2.4^{wet}
2013	80^{warm}	3.6^{dry}	1.4^{dry}
2014	78	4.4	1.9
2015	81^{warm}	4.6	1.7
2016	77	5.4	2.5
2017	65^{cold}	8.3^{wet}	3.0^{wet}
Max	87	8.3	3.4
Min	65	1.5	1.0
Average	76	4.9	2.0
CI 90%	1.9	0.6	0.2

warm - the warmest years by GDD

cold - the coldest years by GDD

wet - the wettest years considering both W and HTC

dry - the driest years considering both W and HTC

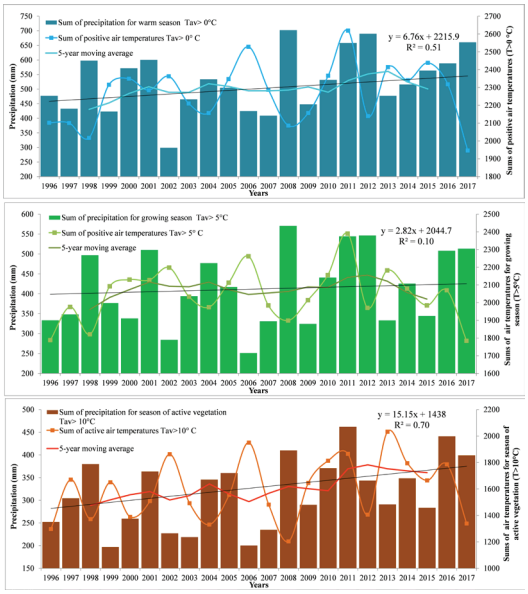

Fig. 3. Sum of annual air temperatures, its 5-year moving average (lines); and sum of annual precipitation (vertical bars) for the following seasons: warm with $T_{av} > 0$°C (blue); growing with $T_{av} > 5$°C (green); active vegetation with $T_{av} > 10$°C (brown).

period, whereas later, the variation came more periodic with 2–3 years of high temperature accumulation interrupted by only one-year low temperature accumulation. There are no statistically significant results for the linear trends of growing degree days (GDD): 5.7°C per year with $p = 0.3$ for warm season, 2.9°C per year with $p = 0.5$ for vegetative season, and 11.1°C per year with $p = 0.15$ for the season of active vegetation.

According to Vorobyev's classification, the climate at SMEAR II with average values $W = 4.9$ and $T = 76$°C falls into gradation with values W between 4.8 and 6.2 (5), T from 64–84°C (c) and belongs to areas with relatively cold temperate and wet climate (class 5c). Fluctuations of T-index were within 65–87°C for 1996–2017, largely within the range prescribed by Vorobyev for the above-mentioned type of climate. Index W was more fluctuating beyond the ranges typical to that type of climate and varied from 1.5 to 8.3. According to this index, the driest years were 2002 and 2006.

Based on the climatic indices, 2008 was characterized as cold and wet, 2011 as warm and wet, and 2006 as extremely warm and dry. However, in 2006, the Vorobyev index was 2.6 indicating enough humidification. Note that the Vorobyev index is developed to classify climate based on the data from the warm season, when $T_{av} > 0$° C, but it is not able to capture conditions for a particular period within the warm season. In the case of summer 2006 (with extreme drought in many sites, see Gao *et al.* 2017), the Selyaninov coefficient (HTC) based on the data from the active growing season (when $T_{av} > 10$°C) showed better results indicating that 2006 was the driest in 22 years. Besides, both the HTC and Vorobyev index selected the same years as dry or wet.

HTC was developed in the former USSR and applied to different climatic zones. This index is deemed not sensitive enough in the boreal zone. However, it should be noted that HTC successfully determined 2006 as the driest year in the existing data set, its value on the verge of sufficient humidity and dry conditions. The index could be applied for boreal forest after the modification of its thresholds for gradations of the local climate.

PAR and its connection to air temperature sums

We selected 2006 for a case study — the year with the driest growing and active vegetation seasons of the study period. The PAR for this year is presented in Fig. 4. We marked the dates of the temperature exceeding thresholds for 0, 5 and 10°C by the vertical lines. In spring, PAR increased gradually but in autumn, it decreased sharply at air temperature threshold 10°C. The highest values of daily PAR at 18 m were observed in summer months with the maximum daily average value ~670 μmol m^{-2} s^{-1}, PAR below canopy (0.6 m) ~180 μmol m^{-2} s^{-1}, reflected PAR (67 m) ~40 μmol m^{-2} s^{-1}, absorbed PAR ~490 μmol m^{-2} s^{-1}. Most absorption of PAR was observed between the spring threshold 0°C and the autumn threshold 10°C, which is a period with a long sunshine duration, increase of LAI (leaf area index) and more intensive process of photosynthesis. As absorbed PAR is dependent on the canopy structure, we expected to see an increase in absorbed PAR during the process of new foliage growth starting at the threshold $T > 5$ °C, reaching its maximum in summer and

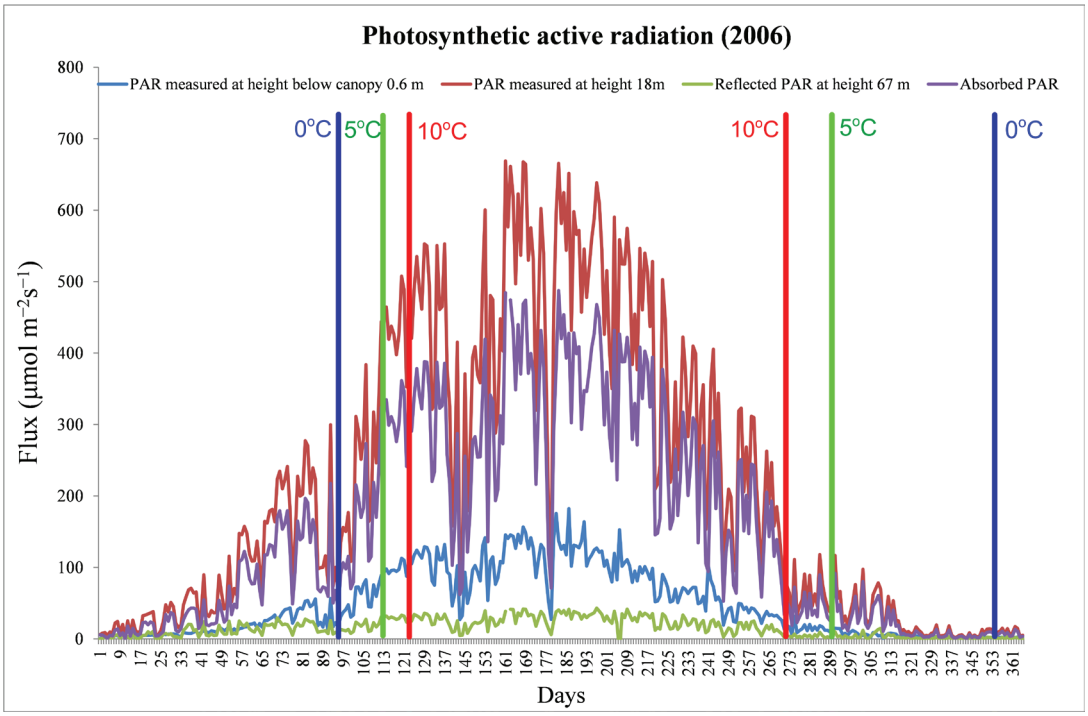

Fig. 4. Annual cycle of average PAR at 0.6 m (blue time series), 18 m (red time series), reflected at 67 m (green time series) and absorbed PAR (violet time series) for year 2006 and dates of air temperature thresholds (vertical lines).

declining in autumn due to the senescence of the oldest needles. However, the amount of PAR varies in time and depends on many factors, especially on cloudiness. The highest decrease in incoming PAR was observed in the end of May and June, the second part of August and first part of September, coinciding with the periods when precipitation was over 10 mm (see Supplementary Information Fig. S3a).

In Supplementary Information Fig. S3a–c, we presented daily absorbed PAR as a percentage of the total PAR for the selected warm and dry year (2006), cold and wet year (2008) and year with typical meteorological conditions (2011). Overall, the behavior of day-to-day variability of absorbed PAR remains similar for selected years, despite differences in the heat and moisture regimes indicated by climatic indices. PAR absorption was more stable within the interval starting when the daily temperature exceeds 5°C and ending when it falls below 10°C, than it was outside of this period. Total variance halved as compared with cold season due to smaller values of incoming PAR and possibly higher measurement uncertainty during cold season. The directional uncertainties of the instrument (LI-190R, LI-COR Inc, USA) exceed 5% at solar zenith angles larger than 70° (directional (cosine) response). In winter, zenith angles are typically large at SMEAR II which likely caused substantial measurements errors. Within the warm season, daily absorbed PAR mostly varied within a 70–85% interval, and the percentage smoothly increased towards the temperature threshold of 10°C in the autumn. We hypothesize that the reason for this increase was the gradually increasing foliage area during this period, corresponding to the growing period of new shoots and needles (Schiestl-Aalto and Mäkelä 2017).

Further, we studied the relation between the sums of absorbed PAR and temperature. The average value of absorbed PAR sum reaches ~35 000 µmol m^{-2} s^{-1} and the standard deviation is ~5600 µmol m^{-2} s^{-1} during the active vegetation season. This is consistent with the high variability in degree-days of active vegetation season with the average values of about 1600°C

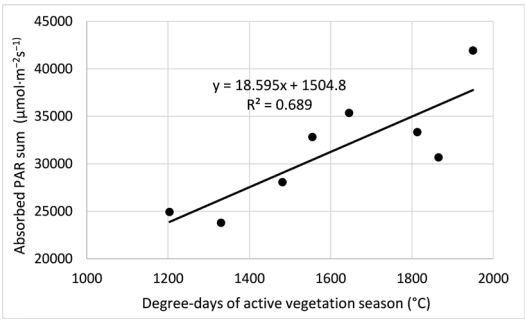

Fig. 5. Dependence of absorbed PAR sum on the degree-days of active vegetation season (p-value < 0.01).

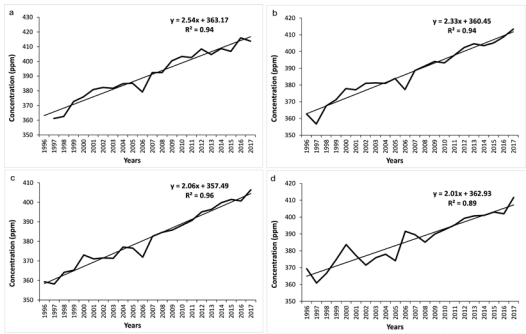

Fig. 6. Mean CO_2 concentrations for (**a**) January, (**b**) April, (**c**) July and (**d**) October at 4.2 m height.

and the standard deviation of about 250°C. Absorbed PAR sums and temperature sums are linearly correlated with the correlation coefficient, r = 0.83 and p-value, p = 0.01 (Fig. 5). In general, both temperature and absorbed PAR depend on cloudiness: accumulated values significantly increase under clear-sky conditions; thus, correlation can be expected. As absorbed PAR sums can be considered as a rough parameterization of forest photosynthetic activity, we can conclude that on an annual basis, temperature sums can also be used to characterize photosynthesis during active vegetation season.

Carbon dioxide concentration and its link to air temperature and PAR

Since the beginning of observations at SMEAR II in 1996, CO_2 monthly mean concentrations measured at 4.2 m have increased from 360 ppm, on average, to 420 ppm (Fig. 6); likewise the observed CO_2 concentration has increased over the planet (IPCC 2021). In July for all years studied, CO_2 concentrations were smaller as compared with other seasons, largely due to high photosynthetic activity of vegetation. However, also the minimum summer CO_2 concentration has a similar strong growing trend of over 2 ppm per year.

Annual cycles of absorbed PAR and atmospheric CO_2 concentrations were plotted (Fig. 7) for the same years 2006 (warm and dry), 2008 (cold and wet) and 2011 (relatively warm and wet). Minimum values of CO_2 concentration were observed in summer (ca. days 153–217) for all three years largely due to active photosynthetic uptake. Absorbed PAR increased simultaneously. Consistently, when temperature decreased below the threshold 10°C in autumn, the concentration of atmospheric CO_2 increased. However, an increase in atmospheric concentration of CO_2 was observed already in late summer — early autumn (ca. days 250–260) 2006 when wildfires in Finland and Eastern Europe released a large amount of burning products (Forest Fires 2009; Leino *et al.* 2014). Note, that the vegetation season of 2006 was characterized by extreme drought in many areas (Spinoni *et al.* 2015): high temperatures and lack of water availability promoted wildfires.

The humid and relatively warm year of 2008 was characterized by the higher atmospheric concentrations of CO_2 compared with 2006, although no significant wildfires were detected in Finland. However, there were fires in Estonia (April–July, strongest in May) and in Sweden (strongest in June, Forest Fires 2009). The annual cycle of CO_2 concentrations in 2008 had similar variations to 2006 with minimum values in late summer. The concentration in 2008 varied from 370 ppm in August to 400 ppm in December.

The warm and wet year of 2011 showed higher fluctuations of CO_2 concentration during the warm season in comparison with the years 2006 and 2008. The minimum value of 375 ppm was observed at the beginning of August 2011 (day 215), and maximum of 426 ppm at the end of August (day 241) with a range of about 50 ppm.

Photosynthesis intensification could be expected due to slight air temperature increase

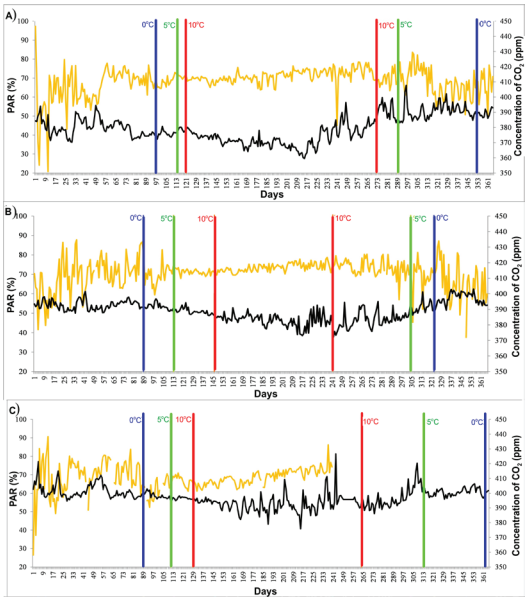

Fig. 7. Annual cycle of daily absorbed PAR (%, yellow) in the layer 18-0.6 m and daily mean CO2 concentrations (ppm, black) at 4.2 m for: (**a**) 2006; (**b**) 2008; and (**c**) 2011 (data gap of PAR described in Methods).

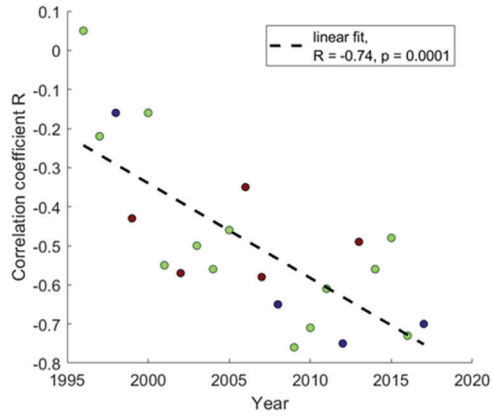

Fig. 8. Increasing negative correlation between years in the daily air temperature and CO_2 concentration. Color code corresponds to wet (blue), dry (red) and normal (green) years in accordance with HTC.

and sustained CO_2 concentration increase of 20–25 ppm per decade. Analysis of intra-annual relations between air temperature and CO_2 concentration showed strengthening in the last years. Overall, the correlation between daily values of air temperature and CO_2 concentration for the whole period 1996–2017 was insignificant (see Supplementary Information Table S4). However, an interesting trend was found when comparing correlation coefficients between years. Before 2000, the correlation coefficients were from -0.10 to -0.43 (p-value $\approx$ 0.2); in early 2000, they varied within -0.50 to -0.60 (p-value < 0.01); and after 2009, the correlation very often became strong with values of about -0.70 to -0.76 (p-value < 0.01). This is illustrated in Fig. 8. We used HTC values to show that dry and wet years had no effect on the connection between the daily air temperature and CO_2 concentration.

Intra-annual relation between daily air temperature and atmospheric CO_2 concentration is negative (negative R-coefficients in Fig. 8), which means that an increase of air temperature results in higher absorption of CO_2. The relation between air temperature and absorption of CO_2 could be affected by an increase in tree biomass, which has more than doubled over the 22 years due to forest growth (Ilvesniemi *et al*. 2009, Launiainen *et al*. 2022). There is also a feedback mechanism between atmospheric CO_2 concentration and photosynthesis. As it was recently revealed, an increase in LAI at SMEAR II was responsible for the observed increase in GPP in the ca. 20-year-long study period, but the increase in atmospheric CO_2 concentration contributed by 30–40% (Launiainen *et al.* 2022). Another factor that might enhance the negative correlation between air temperature and atmospheric CO_2 concentration is the boundary layer height, because the well-mixed boundary layer is typically higher during warm conditions leading to decreased atmospheric concentration of gases within the layer (Huo *et al.* 2021; Zhang *et al.* 2013). It should be also noted that anthropogenic emissions together with air mass origin can affect the correlation between air temperature and atmospheric CO_2 concentration, as was seen in 2006 and 2008 when long-range transport of CO_2 from forest fires was observed.

Conclusions

The most significant changes were found towards the delayed end of the warm season and advanced at the start of the active vegetation

season ($T > 10$°C), totaling 7–8 days per decade. Slight changes were also found at the start of the vegetation season ($T > 5$°C). As a result, the period between 5°C and 10°C had shrunk notably. These shifts result in increasing available temperature resources and change of temperature accumulation within the seasons.

Hydrothermal Vorobyev and Selyaninov indices were calculated for estimating heat and moisture availability for vegetation, which showed a relatively temperate and wet climate, however the year 2006 was extremely warm and dry, and the years 2008 and 2011 were relatively cold and wet. The indices caught features of temperature and humidity distribution, however the existent scale, especially Selyaninov, wasn't sensitive enough to boreal forest in Finland and might need modification to humidity.

The most absorption of PAR was after $T > 0$°C and before $T < 10$°C, which are linked to long sunshine duration, increase of leaf area index and more intensive process of photosynthesis. The fraction of absorbed PAR of total incoming radiation varied within 70–85% and had less variability in the warm season in comparison with the cold season.

Analysis of atmospheric CO_2 concentrations demonstrated a constant increase with a trend 2.0 (October, min. value) — 2.5 ppm per year (January, max. value). In general, concentrations have risen from 360 ppm, on average, to 420 ppm in all seasons. Clear CO_2 concentration increase together with small air temperature increase might influence photosynthetic production, correlation between air temperature and CO_2 concentration strengthened in the last years. Further analysis with multiple sites and multiple years together with ecosystem flux data is needed to draw more solid conclusions.

The results obtained in the study gave evidence to some atmosphere-biosphere interactions in boreal forests under climate change. The prospective of the study is to expand the research on other sites in boreal forests, adding new data, meteorological variables and analysis tools.

Acknowledgements: This paper was written within the framework of project «The Influence of Land cover changes On Atmospheric Boundary Layer and Regional Climate Characteristics». We are thankful to project ENVRIplus which is a part of Horizon-2020 and sponsored by European Commission, for receiving grant to conduct project «The Influence of Land cover changes On Atmospheric Boundary Layer and Regional Climate Characteristics» and for participating in summer school «Formation and Growth of Atmospheric Aerosols», Hyytiälä Forestry Field Station, Finland (13–24 August 2018). We acknowledge the following projects: ACCC Flagship funded by the Academy of Finland grant number 337549, Academy professorship funded by the Academy of Finland (grant no. 302958), Academy of Finland projects no. 1325656, 347782, 316114, 324259 and 325647, "Quantifying carbon sink, CarbonSink+ and their interaction with air quality" INAR project funded by Jane and Aatos Erkko Foundation, European Research Council (ERC) project ATM-GTP Contract No. 742206. The technical and scientific staff in Hyytiälä and SMEAR II station are acknowledged, and the ICOS RI, ACTRIS RI and eLTER RI are gratefully acknowledged for the integrated long-term measurements data set at SMEAR II.

Supplementary Information: The supplementary information related to this article is available online at: http://www.borenv.net/BER/archive/pdfs/ber27/ber27-131-144-supplement.pdf

References

Alonzo M., Andersen H.-E., Morton D. C. & Cook B. D. 2018. Quantifying Boreal Forest Structure and Composition Using UAV Structure from Motion. *Forests* 9: 119.

Arneth A., Makkonen R., Olin S., Paasonen P., Holst T., Kajos M.K., Kulmala M., Maximov T., Miller P. & Shurgers G. 2016. Future vegetation–climate interactions in Eastern Siberia: an assessment of the competing effects of CO_2 and secondary organic aerosols. *Atmos. Chem. Phys.* 16: 5243–5262.

Babst F., Bouriaud O., Poulter B., Trouet V., Girardin M.P. & Frank D.C. 2019. Twentieth century redistribution in climatic drivers of global tree growth. *Science Advances* 5: 4313.

Björheden R. 2021. Climate effects of Forestry in the Nordic-Baltic Region, available at:

Bonan G.B. 2008. Forests and Climate Change: Forcings, Feedbacks, and the Climate Benefits of Forests. *Science* 320: 1444–1449.

Bonan G.B. & Sirois L. 1992. Air Temperature, Tree Growth, and the Northern and Southern Range Limits to Picea mariana. *J. Veg. Sci.* 3: 495–506.

Čirkovs J. 1978. *Lauksaimniecības metroloģijas pamati*. Rīga. Zvaigzne. 186 p.

D'Orangeville L., Houle D., Duchesne L., P. Phillips R. Bergeron Y. & Kneeshaw D. 2018. Beneficial effects of climate warming on boreal tree growth may be transitory. *Nature Comm.* 9: 3213.

Fernández-Martínez M., Vicca S., Janssens I. A., Ciais P., Obersteiner M., Bartrons M., Sardans J., Verger A.,

Canadell J.G., Chevallier F., Wang X., Bernhofer C., Curtis P.S., Gianelle D., Grünwald T., Heinesch B., Ibrom A., Knohl A., Laurila T., Law B.E., Limousin J.M., Longdoz B., Loustau D., Mammarella I., Matteucci G., Monson R.K., Montagnani L., Moors E.J., Munger J.W., Papale D., Piao S.L, & Peñuelas J. 2017. Atmospheric deposition, CO_2, and change in the land carbon sink. *Scientific Reports* 7: 9632.

Findell K.L., Pitman A.J., England M.H. & Pegion P. 2009. Regional and global impacts of land cover change and sea surface temperature anomalies. *J. Climate* 22: 3248–3269.

FMI: Seasons in Finland, available at: Forest Fires in Europe 2008. Report № 9. 2009, available at: Gao Y., Markkanen T., Aurela M., Mammarella I., Thum T., Tsuruta A., Yang H. & Aalto T. 2017. Response of water use efficiency to summer drought in a boreal Scots pine forest in Finland. *Biogeosci.* 14: 4409–4422.

Gauthier S., Bernier P., Kuuluvainen T., Shvidenko A. & Schepaschenko D. 2015. Boreal forest health and global change. *Science* 349: 819-22.

Global forest atlas. Boreal zone, available at:

Hari P. & Kulmala M. 2005. Station for measuring ecosystem-atmosphere relations (SMEAR II). *Boreal Env. Res.* 10: 315–322.

Huo Y., Wang Y., Paasonen P., Liu Q., Tang G., Ma Y., Petäjä T., Kerminen V.-M. & Kulmala M. 2021 Trends of planetary boundary layer height over urban cities of China from 1980-2018, *Front. Env. Sci*. 9: 744255

Ilvesniemi H., Levula J., Ojansuu R., Kolari P., Kulmala L., Pumpanen J., Launiainen S., Vesala T. & Nikinmaa E. 2009: Long-term measurements of the carbon balance of a boreal Scots pine dominated forest ecosystem. *Boreal Env. Res.* 14: 731–753.

IPCC, 2007: Climate Change 2007 – Impacts, Adaptation and Vulnerability. *Contribution of Working Group II to the Fourth Assessment Report of the IPCC*, available at: IPCC, 2013: Climate Change 2013: The Physical Science Basis. *Contribution of Working Group I to the Fifth Assessment Report of the IPCC*, available at:

IPCC, 2018: Global warming of 1.5°C. *Summary for Policymakers*, available at:

IPCC, 2019a: Climate Change and Land. IPCC Special Report on Climate Change, Desertification, Land Degradation, Sustainable Land Management, Food Security, and Greenhouse gas fluxes in Terrestrial Ecosystems. *Summary for policymakers*, available at: IPCC, 2019b: Polar Regions. In: *IPCC Special Report on the Ocean and Cryosphere in a Changing Climate* [H.-O. Pörtner, D.C. Roberts, V. Masson-Delmotte, P. Zhai, M. Tignor, E. Poloczanska, K. Mintenbeck, A. Alegría, M. Nicolai, A. Okem, J. Petzold, B. Rama, N.M. Weyer (eds.)]. Cambridge University Press, Cambridge, UK and New York, NY, USA, pp. 203–320.IPCC, 2021: Climate Change 2021: The Physical Science Basis. Contribution of Working Group I to the Sixth Assessment Report of the Intergovernmental Panel on Climate Change. *Full report*, available at:

Kinnunen R., Lehtonen I., Kas J., Järvelä R., Poutamo H., Wenzlaff C. & Latus J. 2013. Impact of Climate Change on the Boreal Forest in Finland and Sweden. Technical Report. *HENVI Workshop: Interdisciplinary approach to forests and climate change.* 34 p.

Kolari P., Lappalainen H. K., Hänninen H. & Hari P. 2007. Relationship between temperature and the seasonal course of photosynthesis in Scots pine at northern timberline and in southern boreal zone. *Tellus* 59: 542–552.

Kulmala M., Ezhova E., Kalliokoski T., Noe S., Vesala T., Lohila A., Liski J., Makkonen R., Bäck J., Petäjä T. & Kerminen V.-M. 2020. CarbonSink+ Accounting for multiple climate feedbacks from forests. *Boreal Env. Res.* 25:145–159.

Larjavaara M., Lu X., Chen X. & Vastaranta M. 2021. Impact of rising temperatures on the biomass of humid old-growth forests of the world. *Carbon Balance Manage* 16: 31.

Launiainen S., Katul G., Leppä K., Kolari P., Aslan T., Grönholm T., Korhonen L., Mammarella, I., Vesala T. 2022. Does growing atmospheric CO2 explain increasing carbon sink in a boreal coniferous forest? *Global Change Biology* 28: 2910-2929.

Leino K., Riuttanen L., Nieminen T., Dal Maso M.,Väänänen R., Pohja T., Keronen P., Järvi L., Aalto P. P., Virkkula A., Kerminen V.-M., Petäjä T. & Kulmala M. 2014. Biomass-burning smoke episodes in Finland from eastern European wildfires. *Boreal Env. Res.* 19: 275–292.

Majasalmi, T. 2015. Estimation of leaf area index and the fraction of absorbed photosynthetically active radiation in a boreal forest. *Dissertationes Forestales* 187: 52 p.

Makhnykina A. V., Polosukhina D. A., Koshurnikova N. N., Verkhovets S. V. & Prokushkin A. S. 2018. Influence of precipitation on CO_2 soil emission in pine forests of the Central Siberia boreal zone. *IOP Conference Series: Earth and Environmental Science* 211.

Mäki M., Aalto J., Hellen H., Pihlatie M. & Bäck J. 2019a. Interannual and Seasonal Dynamics of Volatile Organic Compound Fluxes From the Boreal Forest Floor. *Front. Plant Sci.* 10:191

Mäki M., Krasnov D., Hellén H., Noe S.M. & Bäck J. 2019b. Stand type affects fluxes of volatile organic compounds from the forest floor in hemiboreal and boreal climates. *Plant Soil*. 441: 363–381.

Massmann, A., Gentine, P. & Lin, C. 2019. When does vapor pressure deficit drive or reduce evapotranspiration? *Hydrol. Earth Syst. Sci. Discuss*.,

Matías L. & Jump A. S. 2014. Impacts of predicted climate change on recruitment at the geographical limits of Scots pine. *J. Experim. Botany* 65: 299–10.

Menzel A., Sparks T. H., Estrella N., Koch E., Aasa A., Ahas R., Alm-Kubler K., Bissolli P., Braslavska O., Briede A., Chmielewski F.M., Crepinsek Z., Curnel Y., Dahl A., Defila C., Donnelly A., Filella Y., Jatczak K., Måge F., Mestre A., Nordli O., Peñuelas J., Pirinen P., Remišová V., Scheifinger H., Striz M., Susnik A., Van Vliet A.J.H., Wielgolaski F.-E., Zach S. & Zust A. 2006. European phenological response to climate change matches the warming pattern. *Global Change Biology* 12: 1969–1976.

OSF, 2017: Official Statistics of Finland (OSF): Greenhouse gases [e-publication]. ISSN=1797-6065. Land

Use, Land-Use Change and Forestry, Preliminary Data 2017. Helsinki: Statistics Finland [referred: 25.6.2022], available at:

Palmroth S. 2009. Boreal Forest and Climate Change – From Processes and Transport to Trees, Ecosystems and Atmosphere. *Silva Fennica* 43: 711–713.

Pauli E., Cermak J., & Teuling A. J. 2022. Enhanced nighttime fog and low stratus occurrence over the Landes forest, France. *Geophys. Res. Lett.* 49: e2021GL097058.

Petäjä T., Tabakova K., Manninen A., Ezhova E., O'Connor E., Moisseev D., Sinclair V. A., Backman J., Levula J., Luoma K., Virkkula A., Paramonov M., Räty M., Äijälä M., Heikkinen L., Ehn M., Sipilä M., Yli-Juuti T., Virtanen A., Ritsche M., Hickmon N., Pulik G., Rosenfeld D., Worsnop D.R., Bäck J., Kulmala M. & Kerminen V.-M. 2022. Influence of biogenic emissions from boreal forests on aerosol–cloud interactions. *Nature Geosci.* 15: 42–47.

Pulliainen J. Aurela M., Laurila T., Aalto T., Takala M., Salminen M., Kulmala M., Barr A., Heimann M., Lindroth A., Laaksonen A., Derksen C., Mäkelä A., Markkanen T., Lemmetyinen J., Susiluoto J., Dengel S., Mammarella I., Tuovinen J.-P. & Vesala T. 2017. *Proc. Nat. Aca. Sci. USA* 114: 11081–11086.

Räty M., Sogacheva L., Keskinen H.-M., Kerminen V.-M., Nieminen T., Petäjä T., Ezhova E. & Kulmala M. 2022. Dynamics of aerosol, humidity, and clouds in air masses travelling over Fennoscandian boreal forests, *Atmos. Chem. Phys. Discuss. [preprint]*, in review.

Rawson H.M., Begg J.E. & Woodward R.G. 1977. The effect of atmospheric humidity on photosynthesis, transpiration and water use efficiency of leaves of several plant species. *Planta* 134, 5–10.

Rousi M. & Heinonen J. 2007.Temperature sum accumulation effects on within-population variation and long-term trends in date of bud burst of European white birch (Betula pendula). *Tree Physiology* 27: 1019–1025.

Ruosteenoja K., Jylhä K. & Kämäräinen M. 2016. Climate Projections for Finland Under the RCP Forcing Scenarios. *Geophysica* 51: 17–50.

Ruosteenoja K, Räisänen J & Pirinen P. 2011. Projected changes in thermal seasons and the growing season in Finland. *Int. J. Clim.* 3: 1473–1487.

Sanderson M., Santini M., Valentini R. & Pope E. 2012. Relationships between forests and weather. *EC Directorate General of the Environment 13th January 2012*, available at: Schiestl-Aalto P. & Mäkelä A. 2017. Temperature dependence of needle and shoot elongation before bud break in Scots pine. *Tree Physiology* 37: 316–325.

Shvidenko A., Buksha I. & Krakovska S. 2018. Vulnerability of Ukraine's forests to climate change. Kyiv. Nika-Centre. P.184.

Shvidenko A., Buksha I., Krakovska S. & Lakyda P. 2017. Vulnerability of Ukrainian Forests to Climate Change. *Sustainability* 9: 1152.

Skrynyk O.A. & Snizhko S.I. 2008. Determination of a stable transition date of air temperature over a fixed value (analysis of methods). *Ukrainian Hydrometeorological Journal* 3, 56–66.

Spinoni J., Naumann G., Vogt J.V. & Barbosa P. 2015. The biggest drought events in Europe from 1950 to 2012. *Journal of Hydrology: Regional Studies* 3: 509-524.

SMEAR concept. Stations measuring earth surface-atmosphere relations, available at: Teuling A.J., Taylor C.M., Meirink J.F., Melsen L.A., Miralles D.G., van Heerwaarden C.C., Vautard R., Stegehuis A.I., Nabuurs G.-J. & de Arellano J.V.-G. 2017. Observational evidence for cloud cover enhancement over western European forests. *Nature Comm*. 8: 14065

Thom D., Rammer W. & Seidl R. 2017. The impact of future forest dynamics on climate: interactive effects of changing vegetation and disturbance regimes. *Ecological Monographs* 87: 665–684.

Vesala T., Suni T., Rannik Ü., Keronen P., Markkanen T., Sevanto S., Grönholm T., Smolander S., Kulmala M., Ilvesniemi H., Ojansuu R., Uotila A., Levula J., Mäkelä A., Pumpanen J., Kolari P., Kulmala L., Altimir N., Berninger F., Nikinmaa E., Hari P. 2005. Effect of thinning on surface fluxes in a boreal forest. *Global Biogeochemical Cycles* 19: GB2001.

Zhang Y., Seidel D. J., & Zhang S. 2013. Trends in Planetary Boundary Layer Height over Europe. *J. Climate*. 26: 10071–10076.